Perspective

Perspective and analysis of ammonia-based distributed energy system (DES) for achieving low carbon community in China

Hui Du,[1] Pengyuan Shen,[2,*] Wai Siong Chai,[1] Dongxue Nie,[1] Chengcheng Shan,[1] and Lei Zhou[1,3,*]

SUMMARY

Carbon reduction in the building sector is crucial in achieving the carbon neutrality goal by 2050. Combined cooling, heating, and power (CCHP) system is a practical technology to achieve energy cascade utilization for building. However, methane usage in the present CCHP system results in carbon dioxide emission, which causes great global warming potential. Ammonia is a non-carbon fuel, implying a potentially powerful measure to achieve carbon neutral burning when serves as fuel for the CCHP system. In this article, we propose the CCHP system that uses ammonia as the fuel source. An ammonia-based distributed energy system (DES) model was developed using brown and green ammonia fuel and an objective function based on ammonia fraction and gas power capacity ratio was proposed. It is found that brown ammonia is more carbon-intensive than green ammonia, but it is cheaper than green ammonia in 2022. However, it is shown that the DES with green ammonia is more economically competitive than brown ammonia by 2050.

INTRODUCTION

Reducing carbon emission is an imperative challenge in this century as it accounts for the global greenhouse effect. As buildings account for almost 50% of the carbon emissions in China as shown in Figure 1, it is vital to save energy and reduce carbon emissions in the building sector (Association, 2021). At the same time, the growth rate of China's carbon emissions has remained at a high level as the beginning of the 21st century (Fan et al., 2015). Therefore, energy efficiency improvement and carbon emissions reduction in the building sector is an indispensable factor in achieving future carbon neutrality.

People have already embarked on attempts in turning to non-carbon-based fuels to curb the trends of rising carbon emission levels in the atmosphere. Among many efforts paid by academia and industry, hydrogen (H$_2$) has emerged as a promising clean energy source because hydrogen-based fuels can offer zero carbon advantages over conventional hydrocarbon fuels. Recently, ammonia (NH$_3$), also a carbon-free molecule, has also come into the vision and has been proposed by researchers as an energy storage media to store and transport as renewable energy. Various ammonia applications have been attempted in industrial and domestic sectors through pure combustion of ammonia or mixed combustion together with hydrogen. As a fuel to achieve carbon neutrality targets, another potential application for ammonia is its use in distributed energy systems (DES) in the building sector.

As we know, the life cycle analysis (LCA) of a building provides a clear picture of a building's carbon footprint, including phases of construction, commissioning, operational, maintenance, and decommissioning. The operational phase of the building has the highest carbon emissions among all phases (Beccali et al., 2013). DES are small-scale energy production technologies located close to the end-users to provide onsite energy according to building energy demands, which can be a potential maneuver to whittle carbon emission during the building operation phase (Zhou et al., 2013). Interest in the development of DES is intensifying in China because of the advantages of its high overall efficiency, low energy transmission losses, and low overall negative environmental impact. Traditionally, DES are fueled by fossil energies such as coal and methane (CH$_4$), which produces large amounts of greenhouse gas (GHG) emissions if exhausts are not sequestered, while the application of ammonia/hydrogen, a comparatively clean fuel free of global warming potential, in the DES has rarely been reported.

[1]School of Mechanical Engineering and Automation, Harbin Institute of Technology, Shenzhen, Shenzhen, Guangdong 518055, China

[2]School of Architecture, Harbin Institute of Technology, Shenzhen, Shenzhen, Guangdong 518055, China

[3]Lead contact

*Correspondence:
shenpengyuan@hit.edu.cn (P.S.), l.zhou@hit.edu.cn (L.Z.)
https://doi.org/10.1016/j.isci.2022.105120
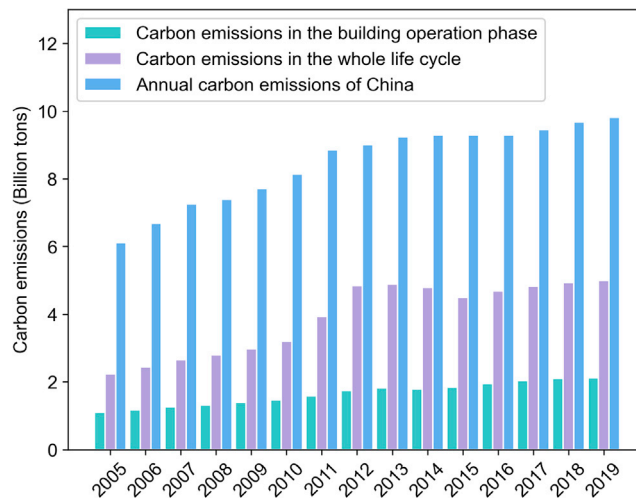
Figure 1. Total building carbon emissions and its percentage of total carbon emissions in China from 2005 to 2018

Various studies have shown that using pure ammonia as the fuel improves overall efficiency and generates less NO_x emission reduction, including gas turbines (Guteša Božo et al., 2021; Kurata et al., 2017; Valera-Medina et al., 2017b, 2019; Yapicioglu and Dincer, 2018), CCHP technologies (Ghorbani et al., 2021; Parikhani et al., 2020; Wang et al., 2017) and furnaces (Ishihara et al., 2020; Murai et al., 2017; Tamura et al., 2020; Zhang et al., 2020). Ammonia co-firing with hydrogen or methane can drive power equipment such as boilers and gas turbines, thereby powering the energy-efficient DES. In the case of furnaces/boilers, ammonia co-firing with other fuels is an effective way to keep the heat transfer constant and reduce NO_x generation (Tamura et al., 2020). The ammonia-based internal combustion engine can be used to limit the carbon footprint and decrease GHG emissions (Bicer and Dincer, 2018). Gas turbines fueled by ammonia can be employed in energy production and provide combined cooling, heating, and power (CCHP) in the DES. Studies (Valera-Medina et al., 2019; Valera-Medina et al., 2015, 2017b) on the application of ammonia-hydrogen blends in gas turbines have shown that ammonia-hydrogen can improve overall efficiency and reduce NO_x emissions to a level that is lower than the current EU standard threshold (Guteša Božo et al., 2021). The required district heating is provided by the heat generated by the boiler and the waste heat of the gas generator through the heat exchange device, while the district cooling can also be provided by making use of the medium temperature heat rejection together with lithium bromide absorption units.

Methane has a higher heating value with high carbon emission during combustion compared to ammonia. In contrast, ammonia combustion produces no carbon emission, which is cleaner and more environmentally friendly than methane and its low price makes the use of ammonia as a fuel for DES more attractive. Moreover, as a hydrogen carrier, which is also a clean energy source, the combination of ammonia with hydrogen improves the heating value and the combustion rate of pure ammonia, ensuring a stable energy supply for DES. Studies on the combustion characteristics of ammonia-hydrogen and ammonia-methane have been widely reported (Bao et al., 2022; Otomo et al., 2018; Tang et al., 2021; Valera-Medina et al., 2017a), with their main properties available in the reference (Chai et al., 2021).

In this article, we begin with evaluating the ammonia potential and usage as a carbon-free energy source in the DES system, including a more in-depth discussion of the carbon emission, NO_x emission, and economical aspects based on life cycle analysis. The shortcomings and challenges of single ammonia energy source usage in DES are discussed. In view of these points, we consider combining ammonia with a currently available energy source (methane) and another carbon-free fuel (hydrogen) to resolve the shortcomings mentioned and build an analytical model to evaluate the overall picture of carbon emission and economic performance under different scenarios. The city of Shenzhen and Harbin in China are chosen as the representative cities in this evaluation. Moreover, recognizing the need to fully understand the potential and implication of ammonia usage in DES, we discuss the potential of ammonia's competence in decarbonization and economic performance in China.
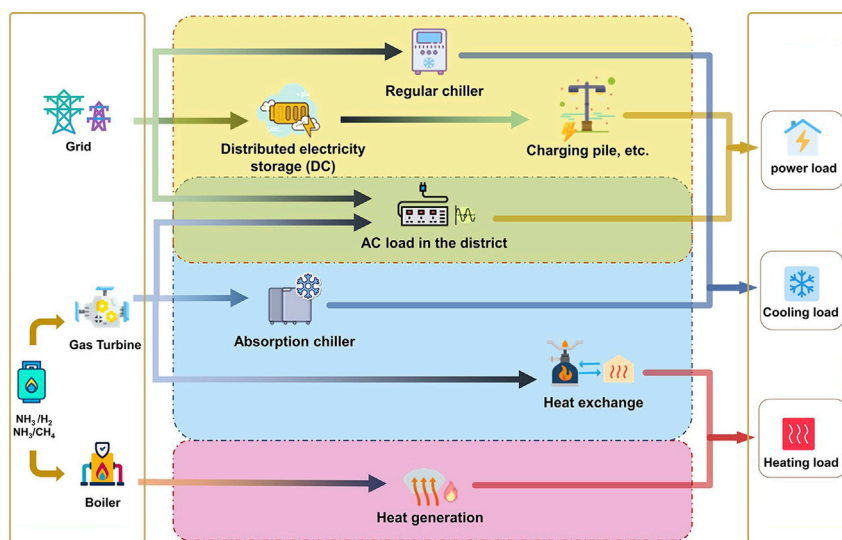
Figure 2. Ammonia-based CCHP system

METHODOLOGY

The CCHP system in DES can be achieved through ammonia combustion and the ammonia-based DES model is built to perform emission and economic analysis in this research. As shown in Figure 2, the CCHP system in the model consists of three main components: heat engine system, heat recovery system, and absorption chiller system. In this study, a gas turbine is used as the generator. The high-temperature exhaust gas after power generation is first sent to an absorption chiller for cooling, and the remaining heat is fed to a plate heat exchanger for space heating and domestic hot water heating. In addition, the system is equipped with boilers and regular chillers to ensure that the CCHP system can meet the heating and cooling needs of the district. The alternating current generated by the generator can meet part of the electricity demand and it is assumed that any DES undersupplied electricity can be purchased from the grid. Owing to the difficulties in connecting DES surplus electricity to the grid in practical applications, DES surplus electricity is assumed not to be sold to the grid. If the heat recovered meets the instantaneous hot and cold demand, the surplus heat will be released directly into the environment. The CCHP system is also equipped with a battery bank that uses low-cost electricity at night to meet some direct current demands. In this research, the amount of cooling, space heating, and domestic hot water heating supplied by the gas turbine can be determined based on an hourly load of the buildings in the district. The proposed framework helps to minimize the annualized heating and cooling cost per square meter (HC) of the local energy system during its life cycle considering its electricity, heating, cooling, and hot water loads, fuel prices, technical and financial constraints of the available technologies.

Two kinds of fuel mixtures, NH_3/CH_4 and NH_3/H_2, are studied for ammonia application in the DES model. Ammonia can be grouped into five categories depending on the energy source of ammonia production, mainly determined by its source production method, hydrogen. It is labeled as brown and gray ammonia if the hydrogen is made from coal gasification and natural gas reforming, respectively. Blue ammonia is prepared similarly to brown and gray ammonia, with additional carbon capture and storage unit. Green ammonia is produced entirely from renewable electricity, whereas hydrogen is from electrolyzer stacks. Another category is pink ammonia (nuclear-based ammonia synthesis) (Boero et al., 2021), which has the lowest global warming potential (0.09 t CO^2-eq/t NH_3) (Bicer and Dincer, 2017). Brown and green ammonia are included in this study as hydrogen from coal gasification account for 63.54% of hydrogen production in China (Liu et al., 2022), and the entirely electrochemical, renewable energy-powered green ammonia synthesis technology is expected to dominate in the future (MacFarlane et al., 2020). Blue ammonia, which has no economic advantage with carbon capture and storage units (Oni et al., 2022), gray and pink ammonia, accounting for a relatively small amount in China (Liu et al., 2022), were not included in this study.

In this study, Shenzhen and Harbin, which are the southernmost and northernmost metropolis of China are selected as the case studies of ammonia-based DES. They represent two interesting cases of southern and
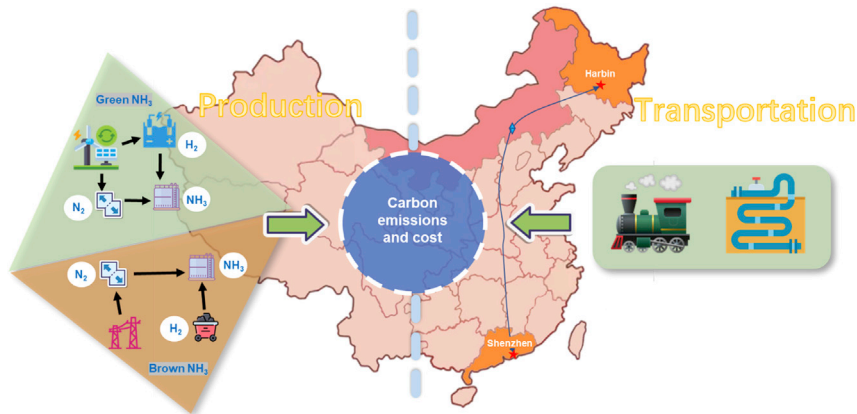
Figure 3. Carbon emissions and costs from the production and transportation of fuels

northern climates in China, respectively, which is conducive to the understanding of the performance of DES in distinct climate conditions. Shenzhen has a "hot summer and warm winter" climate while Harbin has four distinct seasons with long, cold winters and short, cool summers.

At present, more than 90% of the ammonia produced in the world is obtained through the Haber-Bosch process (Gálvez et al., 2007). The Haber-Bosch process uses hydrogen produced from fossil energy and N_2 separated from the air as raw materials to produce ammonia, which accounts for more than 90% of ammonia production in China (Giddey et al., 2017; Liu et al., 2022; Smith et al., 2020). Both ammonia production process and the transportation phase generate carbon emissions (Al-Breiki and Bicer, 2021). As there is fuel consumption during ammonia transportation, a certain amount of carbon emission will be generated at this stage, in addition to the labor and transportation carrier costs, which will eventually be reflected in the overall ammonia cost. For longer transport distances, our model includes the carbon emissions and transportation costs of ammonia. Similarly, the carbon emissions and transportation costs of hydrogen should be fully considered owing to the more demanding conditions of transportation. The model only covers carbon emissions and costs from fuel production and transportation processes, but those of storage processes are ignored owing to the assumption of *in situ* use for DES as shown in Figure 3.

The case study assumes a medium-scale building complex made up of different building types, including office, shopping malls, and hotels, with a total building area of 1,444,600 m^2 in both cities using typical meteorological year weather data (Theuri, 2008) for building energy use simulation. The building energy model is constructed in EnergyPlus (Crawley et al., 2000) for detailed building energy simulations to provide an energy demand profile of the district energy system in this study, with reference to International Energy Conservation Code 2015 (Council et al., 2000) for the buildings. Later, our DES model computes the combustion and economic performance of ammonia-based fuels under relevant conditions. Based on the data from the literature review (Fasihi et al., 2021; Gu et al., 2020; Shi et al., 2020), the years 2022 and 2050 are chosen for economic analysis as the benchmark for the current and future technology, in which the latter stands for the year of targeted global net zero carbon emission (Fasihi et al., 2021; Janssen et al., 2022). 2050 is the year in which the Paris Agreement (Agreement, 2015) calls for net zero by 2050, which means that greenhouse gas emissions are reduced to as close to zero as possible and any remaining emissions are reabsorbed from the atmosphere, for example by the oceans and forests. In China, 2050 means being on track to achieving China's carbon neutrality goal 10 years earlier.

Briefly, the optimization model obtains an optimized DES configuration by minimizing the annualized life cycle heating and cooling cost per square meter (*HC*) as follows.

$$HC = \left(IC_{tol} + C_{plug} - R_{elec} + C_{hc\_purchase} \right) \Big/ A \qquad \text{(Equation 1)}$$

where IC_{total} is the total investment cost, C_{plug} is the cost for plug loads from the grid, R_{elec} is the revenue of the electricity, $C_{hc\_puchase}$ is the cost of purchased heating and cooling, and A is the area of the project in each city.

Another main objective is to calculate the total carbon emissions (CE_{total}) by the following equation.

$$CE_{total} = (CE_{elec} + CE_{gas})/A \qquad \text{(Equation 2)}$$

where CE_{elec} is the carbon emissions generated during the production and use of electricity, CE_{gas} is the carbon emissions from the mixture of gases consumed by the DES system. The input parameters of the ammonia-DES are listed in Table 1.

The largest contributor to the cost of green ammonia production is the cost of green hydrogen production (del Pozo and Cloete, 2022; Salmon and Bañares-Alcántara, 2021). In the future, the cost of renewable energy generation will decrease, and the electrolyzer efficiency and system lifetime will increase, the cost of green ammonia production is expected to decrease accordingly (Roos, 2021).

This study aims to optimize the CCHP system by adjusting the value of the generator power capacity ratio ($GPCR$), as shown in Equation (3), which is set to 0 to 50%.

$$GPCR = P_{gen}/L_{peak} \qquad \text{(Equation 3)}$$

where P_{gen} is the ratio of gas generator output power, and P_{peak} is the peak electricity power load. The volume fraction of ammonia in the fuel mixture in the model ranges from 0% to 100%. As a result, HC and carbon emissions are functions of NH_3 volume fraction and $GPCR$. A detailed description of the DES model is found in the STAR Methods section.

RESULTS AND DISCUSSION

Brown ammonia

At present, the main source of ammonia is brown ammonia, which is mainly produced by coal gasification (Salmon and Bañares-Alcántara, 2021). Annualized carbon emissions from brown ammonia mixed with CH_4 or H_2 in Harbin and Shenzhen are shown in Figure 4. In total, annualized carbon emissions increase with NH_3 volume fraction for all cases, because brown ammonia is sourced from coal gasification, a greater share of ammonia in the fuel mixture results in more carbon emissions. An increase in $GPCR$ also leads to increased annualized carbon emissions, because a higher $GPCR$ means a higher ratio of generator output power to the peak electricity load, resulting in more carbon emissions. Brown ammonia occupies the highest annualized carbon emissions at 100% NH_3 volume fraction in the mixture, 543.56 kg/(m^2·y) in Harbin and 334.99 kg/(m^2·y) in Shenzhen at 50% $GPCR$. The lowest annualized carbon emissions at 0% NH_3 volume fraction show that brown ammonia as a fuel does not reduce carbon emissions but rather increases them. Harbin has the maximum carbon emissions from NH_3/H_2 mixture (Figure 4B), while Shenzhen has the minimum carbon emissions from NH_3/CH_4 mixture (Figure 4C). By comparing fuel types, NH_3/H_2 has higher annualized carbon emissions than NH_3/CH_4 because the hydrogen source from brown ammonia is produced from coal gasification, while methane is produced from natural gas and has a lower carbon footprint than hydrogen from coal gasification. Harbin has higher annualized carbon emissions than Shenzhen, as Harbin has a greater heating demand in winter.

Annualized HC from brown ammonia mixed with CH_4 or H_2 in Harbin and Shenzhen is shown in Figure 5. HC estimates for brown ammonia are based on current technology and costs. Overall, a higher $GPCR$ corresponds to a higher HC for a given percentage of ammonia in the fuel mixture as a higher $GPCR$ represents more cost for consuming more fuel. The exception is the case of the NH_3/CH_4 mixture in Shenzhen (Figure 5C), where the HC peaks with $GPCR$ at about 55% of ammonia because the cost generated by fuel is exceeds that of purchased electricity when the NH_3 volume fraction is greater than 55%. Harbin NH_3/H_2 has the highest HC value, while Shenzhen NH_3/CH_4 has the lowest HC value. In Harbin and Shenzhen, the highest HC values for NH_3/H_2 mixtures are RMB ¥589.78/(m^2·y) and RMB ¥435.41/(m^2·y), respectively. By comparing the fuel types, HC corresponding to NH_3/H_2 blends is higher than that of NH_3/CH_4 blends, mainly owing to that the H_2 price from coal gasification is higher than CH_4. Similar to carbon emissions, HC is higher in Harbin than in Shenzhen, because Shenzhen's cooling demand is about 1.5 times higher than Harbin's, while Harbin's heating demand is about 3 times higher than Shenzhen's.

Green ammonia

In the future, it is envisioned that the ammonia source will mainly come from green ammonia, which is produced from renewable energy sources (MacFarlane et al., 2020). The annualized carbon emissions of green

Table 1. Input parameters from the literature

Item	Unit	Value(s)	Reference(s)
Grid price in Harbin	RMB¥/kWh	0.25–0.75	(Commission, 2022; State Grid Heilongjiang Electric Power Co., 2021)
Grid price in Shenzhen	RMB¥/kWh	0.25–1.03	(China Southern Power Grid Ltd., 2022)
Boiler Efficiency	%	89.59–80.52	(Kim et al., 2021)
NH_3 Lower heating value	MJ/kg	18.6	(Standards and Technology, 2017)
H_2 Lower heating value	MJ/kg	120	(Standards and Technology, 2017)
CH_4 Lower heating value	MJ/kg	50	(Standards and Technology, 2017)
Generator efficiency for NH_3/H_2	%	33.7–34.4	(Gill et al., 2012)
Generator efficiency for NH_3/CH_4	%	37.4–46.2	(Ishaq and Dincer, 2020)
Brown ammonia production cost (2022)	$/kg	0.43	(Fasihi et al., 2021)
Green ammonia production cost (2022)	$/kg	0.65	(Fasihi et al., 2021)
Green ammonia production cost (2050)	$/kg	0.32	(Fasihi et al., 2021)
Ammonia transport cost by trains	$/ton/km	0.04	(Cardoso et al., 2021)
Brown hydrogen production cost (2022)	$/kg	1.63	(Gu et al., 2020)
Green hydrogen production cost (2022)	$/kg	3.59	(Shi et al., 2020)
Green hydrogen production cost (2050)	$/kg	2.18	(Janssen et al., 2022)
Hydrogen transport cost by trucks (Shenzhen)	$/kg	4.54	(Gu et al., 2020)
Hydrogen transport cost by trucks (Harbin)	$/kg	3.22	(Gu et al., 2020)
Methane import cost	$/MJ	0.0036–0.0133	(Zhang et al., 2021)
Carbon footprints of coal fired plant	g/kWh	810.35	(Zhao et al., 2017)
Carbon footprints of a wind farm	g/kWh	12.51	(Zhao et al., 2017)
Brown ammonia production carbon emissions	kg of CO_2 eq/kg of NH_3	4.44	(Zhang et al., 2019)
Green ammonia production carbon emissions	kg of CO_2 eq/kg of NH_3	0.42	(Wu et al., 2021)
Ammonia transportation carbon emissions (Shenzhen)	kg of CO_2 eq/kg of NH_3	0.17	(Osorio-Tejada et al., 2022)
Ammonia transportation carbon emissions (Harbin)	kg of CO_2 eq/kg of NH_3	0.12	(Osorio-Tejada et al., 2022)
Brown hydrogen production carbon emissions	kg of CO_2 eq/kg of H_2	20	(Gu et al., 2020)
Green hydrogen production carbon emissions	kg of CO_2 eq/kg of H_2	1.19	(Shi et al., 2020)
Hydrogen transportation carbon emissions (Shenzhen)	kg of CO_2 eq/kg of H_2	1.02	(Gu et al., 2020)
Hydrogen transportation carbon emissions (Harbin)	kg of CO_2 eq/kg of H_2	0.72	(Gu et al., 2020)
Methane transportation carbon emissions	g of CO_2 eq/GJ.km	1.35	(Di Lullo et al., 2020)
Methane production carbon emissions	g CO_2-eq/MJ	24.4	(Zhang et al., 2021)
NO_x emissions for NH_3/CH_4	ppm	638–3,060	(Rocha et al., 2019)
NO_x emissions for NH_3/H_2	ppm	5,894–14,250	(Rocha et al., 2019)

ammonia mixed with CH_4 and H_2 in Harbin and Shenzhen regions, respectively, are shown in Figure 6. For green ammonia, the decrease in carbon emissions with NH_3 volume fraction and *GPCR* suggests that the use of more green ammonia in DES systems can significantly reduce carbon emissions. It is noteworthy that for the case of NH_3/H_2 in Shenzhen (Figure 6D), carbon emissions, although reduce overall for a given *GPCR* scenario, increase slightly with NH_3 volume fraction, because ammonia emits more carbon per unit volume than hydrogen over its entire life cycle. NH_3/CH_4 produces the most carbon emissions in Harbin, while NH_3/H_2 results in the least carbon emissions in Shenzhen. The highest annualized carbon emissions are in the NH_3/CH_4 mixture, where Harbin is 297.71 kg/(m²·y) in the 0% NH_3 volume fraction and 0% *GPCR* scenario, and that in Shenzhen is 143.22 kg/(m²·y) in the 0% NH_3 volume fraction and 50% *GPCR* scenario. Similar to brown ammonia, the carbon emissions from Harbin are higher than those from Shenzhen. Carbon emissions from NH_3/CH_4 mixture are also higher than NH_3/H_2 mixture owing to the fact that burning CH_4 itself produces CO_2. A comparison of the carbon emissions of green ammonia (Figure 6) and brown ammonia (Figure 4) shows that the carbon emissions of green ammonia are almost halved, suggesting that green ammonia produced from renewable energy sources would be a prime candidate for achieving carbon neutrality.
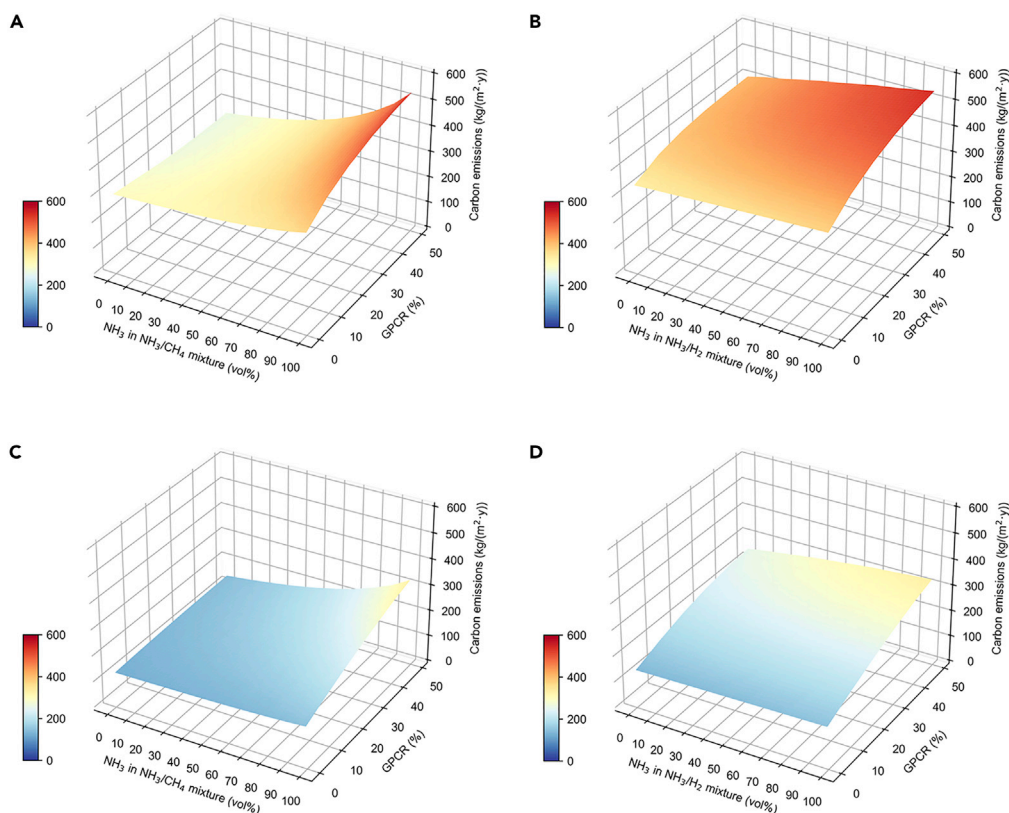
Figure 4. Carbon emissions from brown ammonia

(A) For NH3/CH4 mixture in Harbin.

(B) For NH3/H2 mixture in Harbin.

(C) For NH3/CH4 mixture in Shenzhen.

(D) For NH3/H2 mixture in Shenzhen.

The results of the analysis of the economics of green ammonia in 2022 are shown in Figure 7. The increase in *HC* with *GPCR* in Figures 7A, 7B, and 7C shows that the use of ammonia is not yet economical with the current technology. One exception to NH_3/CH_4 in Shenzhen is that as the *GPCR* increases, *HC* decreases below about 40% of ammonia and increases at greater than 40%. Compared with brown ammonia, green ammonia has a higher *HC* than brown ammonia in 2022. The economic analysis of green ammonia shows that in 2022, *HC* up to RMB ¥767.43/($m^2 \cdot y$) in Harbin and RMB ¥575.02/($m^2 \cdot y$) in Shenzhen, when NH_3 volume fraction is 0% and *GPCR* is 50%. Similar to brown ammonia, *HC* in Harbin is higher than in Shenzhen. The fact that NH_3/H_2 always costs more than NH_3/CH_4 for a given city suggests that it is not yet economical with current technology despite giving off lesser carbon emissions.

In the future, it is predicted that the price of green ammonia decreases with the advancement of renewable energy technologies (Franco et al., 2021). The *HC* predicted using the future price of green ammonia is shown in Figure 8. Comparing the green ammonia 2022 and 2050 prices reveals that in all cases the corresponding *HC* is lower in 2050. The annualized maximum value of *HC* corresponding to green ammonia is projected to decrease to RMB ¥603.45/($m^2 \cdot y$) in Harbin and RMB ¥442.76/($m^2 \cdot y$) in Shenzhen, in a scenario where NH_3 volume fraction in NH_3/H_2 is 0% and *GPCR* of 50%. Green ammonia in 2022 is not economical at today's cost, which is consistent with related studies (Cesaro et al., 2021; Fasihi et al., 2021; Nayak-Luke and Bañares-Alcántara, 2020; Salmon and Bañares-Alcántara, 2021; Zhang et al., 2021). The comparison of Figures 5 and 8 reveals that the price of *HC* corresponding to green ammonia 2050 is lower than that of brown ammonia, indicating that green ammonia will be highly economical in the future.

The analysis of the above results shows that green ammonia not only has the advantage of low carbon emissions but also has advantages in terms of future costs. For clarity of illustration, Figure 9 is drawn in
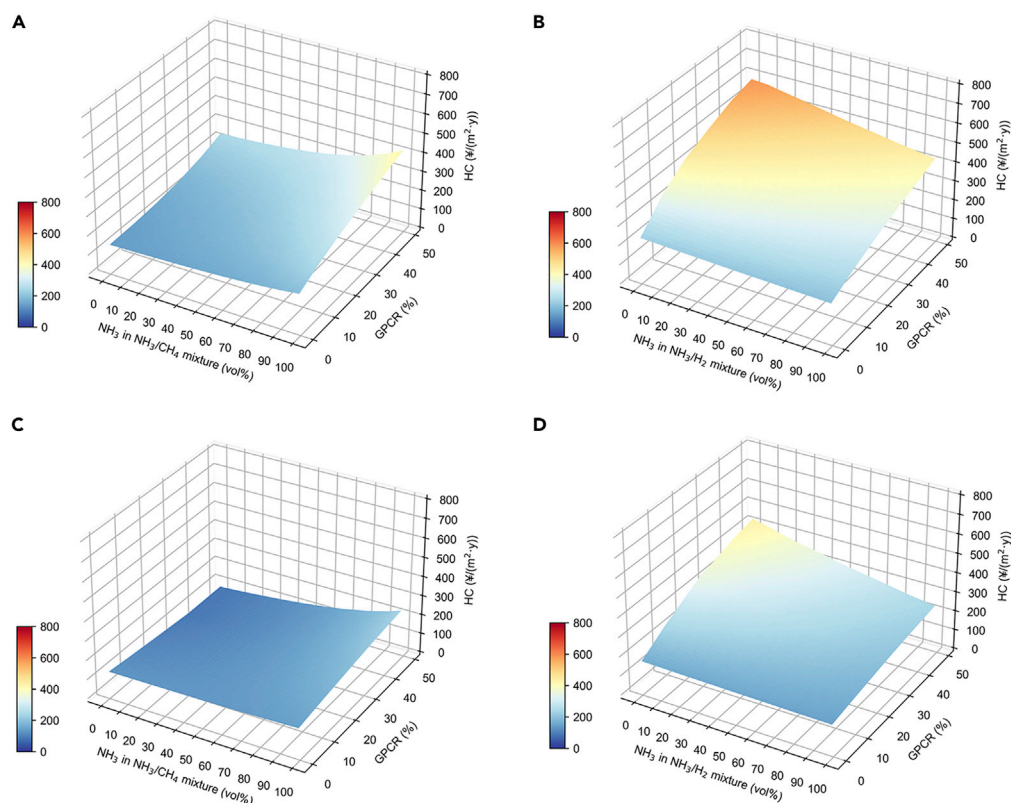
Figure 5. Heating and cooling cost per square meter from brown ammonia
(A) For NH3/CH4 mixture in Harbin.
(B) For NH3/H2 mixture in Harbin.
(C) For NH3/CH4 mixture in Shenzhen.
(D) For NH3/H2 mixture in Shenzhen.

order to compare the relationship between carbon emissions and *HC*. As mentioned previously, for a given *GPCR*, carbon emissions decrease with NH_3 volume fraction, indicating that the green ammonia addition is effective in reducing carbon emissions. The *HC* trend varies, as the NH_3 volume fraction in the fuel mixture increases, with the *HC* decreasing in NH_3/H_2 case but increasing in NH_3/CH_4 case. Although NH_3/H_2 has a significant carbon reduction effect, the *HC* corresponding to NH_3/H_2 is higher than NH_3/CH_4 for the same *GPCR* in a given city, suggesting that a satisfactory application of NH_3/H_2 in the future will require technological advances in green ammonia production which resulting in much lower costs.

Comparison of green and brown ammonia

To compare green and brown ammonia, Figures 10 and 11 show the carbon emissions and HC for *GPCR* from 0% to 50% in Harbin and Shenzhen, respectively. Again, the carbon emission of brown ammonia is found to increase with NH_3 volume fraction while the opposite trend is observed for green ammonia. The greater the green ammonia fraction in the fuel mixture, the greater the reduction in carbon emissions and cost. The *HC* corresponding to green ammonia is also lower than brown ammonia for either *GPCR* at the same volume fraction of ammonia. At the maximum *GPCR* (Figures 10F and 11F), 100% green NH_3 volume fraction is able to reduce carbon by 71.55 and 74.77% compared to brown ammonia, and the *HC* of green ammonia is also 16.81 and 19.23% lower than brown ammonia, for Harbin and Shenzhen, respectively. In addition, city-to-city comparisons show that carbon emissions in Harbin are 1.62 and 1.83 times higher than carbon emissions in Shenzhen for brown and green ammonia, respectively, at 100% NH_3 volume fraction and 50% *GPCR*. *HC* in Harbin is 1.79 times and 1.85 times higher than *HC* in Shenzhen, respectively, for brown and green ammonia under the same conditions.
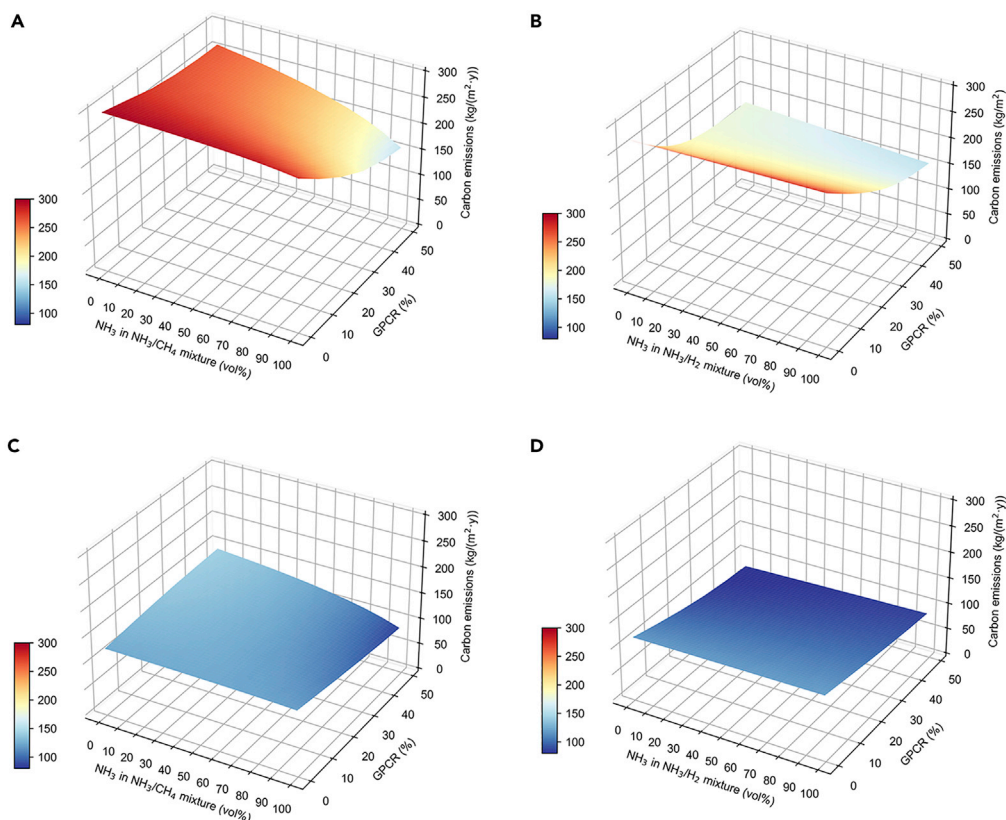
Figure 6. Carbon emissions from green ammonia
(A) For NH3/CH4 mixture in Harbin.
(B) For NH3/H2 mixture in Harbin.
(C) For NH3/CH4 mixture in Shenzhen.
(D) For NH3/H2 mixture in Shenzhen.

NO_x emissions

NO_x emissions are one of the major concerns as ammonia is a nitrogenous fuel. As NO dominates in the NO_x emissions, therefore this article focuses on NO. As the validated experimental model (Rocha et al., 2019) included a range of 30-80% ammonia volume fractions, this range of ammonia fractions is assumed in this study. As shown in Figure 12, with a certain percentage of NH_3, NO_x emissions increase with the *GPCR* for all cases. In ammonia-containing flames, NO generation is the result of a combination of thermal NO and fuel NO, so it is necessary to consider NO generation from both pathways. For NH_3/CH_4 mixture, NO_x emissions peak at a certain NH_3 volume fraction for a given *GPCR*. NO_x increases first because more fuel NO_x is generated by combustion as NH_3 becomes more abundant, and the higher flame temperature promotes NH_3 combustion and N_2 cracking. Fuel NO is more sensitive to the increase of total NO emission while the ammonia ratio is below the critical point (Xiao et al., 2017). As the NH_3 ratio increases, the NH_i radicals in the flame gradually increase, which can promote the generation of fuel NO. However, when the NH_3 volume fraction is high (>65% in this study), the lower fuel heating value lowers the flame temperature, inhibiting the NO forward reaction, so that the fuel NO_x becomes less. Furthermore, considering the "DeNO$_x$ing" effect from $NH_2+NO \leftrightarrow H_2O + N_2$, as the NH_3 ratio exceeds a critical point, NO reacts with excess NH_i radicals and is thus consumed (Tian et al., 2009; Xiao et al., 2017). It explains the trend of why NO emissions increase first and then decrease with the increase of the ammonia ratio. For the NH_3/H_2 mixture, the flame temperature of NH_3/H_2 is higher than that of NH_3/CH_4. As the NH_3 volume fraction increases, the NO_x emission first decreases because of the decreased thermal NO_x as flame temperature decreases and then increases because of the increased fuel NO_x. The production of NO is mainly related to free radicals such as H, OH, and HNO, ($NO_2 + H \leftrightarrow NO + OH$, $HNO + H \leftrightarrow NO + H_2$ and $HNO + OH \leftrightarrow NO + H_2O$). With the increase in H_2 ratio, the generated NO increases rapidly through these reaction pathways, which explains the high NO emissions at low ammonia ratio (Nozari and Karabeyoğlu, 2015). Although the ammonia ratio is above the critical point scenario, NO increases with the ammonia ratio
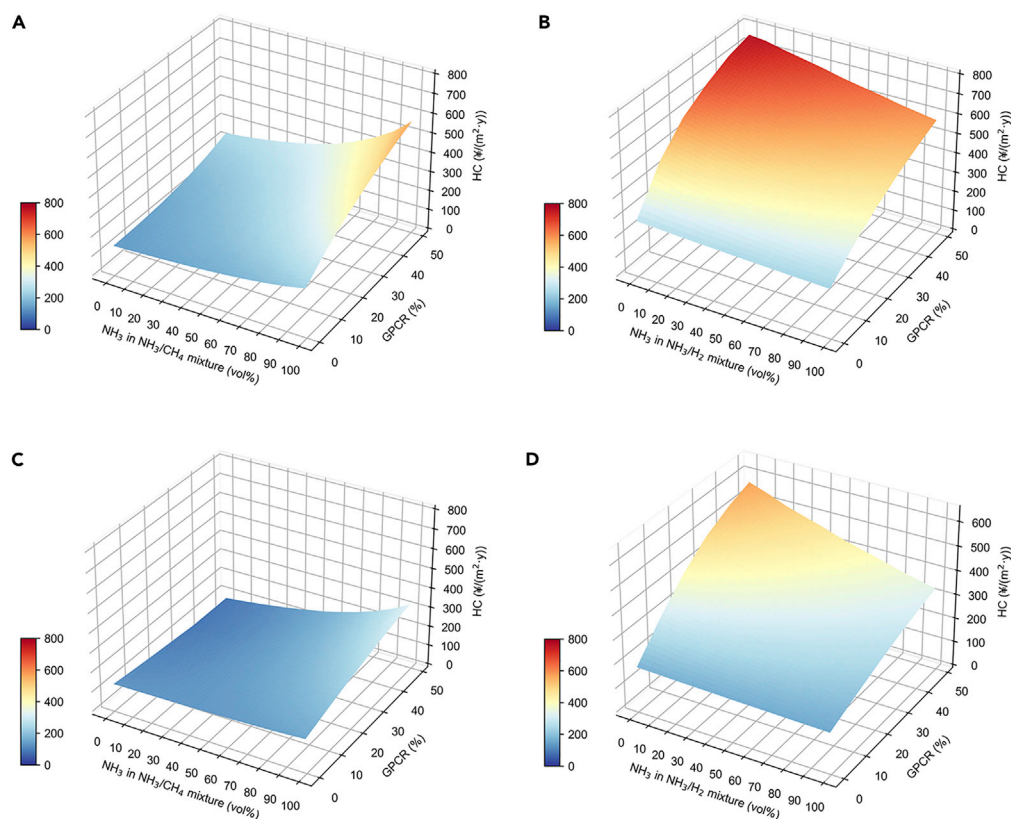
Figure 7. Heating and cooling cost per square meter from green ammonia in 2022
(A) For NH3/CH4 mixture in Harbin.
(B) For NH3/H2 mixture in Harbin.
(C) For NH3/CH4 mixture in Shenzhen.
(D) For NH3/H2 mixture in Shenzhen.

because it dominates in the fuel mixture and producing more fuel NO. On average, NO_x emissions from NH_3/H_2 mixture are 5.67 times larger than NH_3/CH_4 mixture in Harbin and 5.98 times larger in Shenzhen. The NO_x emissions of Harbin are 6.77 times larger than those of Shenzhen for the NH_3/CH_4 mixture and 6.39 times larger for the NH_3/H_2 mixture.

Sensitivity analysis

Natural gas prices, hydrogen prices, ammonia prices, and electricity prices that have impacts on DES costs were studied as input parameters for sensitivity analysis by using the Morris method (Morris, 1991). The Morris method assesses the elementary effects resulting from changes in the input parameters at different sample points. Morris mean elementary effect μ, absolute of the mean elementary effect μ^* and SD of the elementary effect σ are plotted to identify the influential and non-influential inputs for green ammonia in 2050 (see Figure 13). Sensitivity analysis of *HC* in green ammonia 2022 and brown ammonia is attached in Supplemental information (see Figures S1 and S2). Bars with larger mean values indicate more variable effects of the input parameters on the *HC* (end-user cost of DES). Bars with high standard deviations indicate non-linearity and/or interactions between the input parameters. The black lines are the bootstrapped confidence intervals for the absolute of the mean elementary effect. The electricity price is with the maximum μ and σ regardless of the case settings, indicating that it has a significant impact on the economic performance of the DES. Smaller μ for ammonia price, natural gas price, and hydrogen price indicate that the *HC* results are comparatively less sensitive to these parameters.

Violin plots are plotted to depict the probability distribution of *HC* variation with economic parameters for green ammonia in 2050 for all cases (see Figure 14). The width of the box indicates the kernel density of *HC*, and the white dots indicate the mean *HC* with error bars indicating 95% confidence intervals. The mean
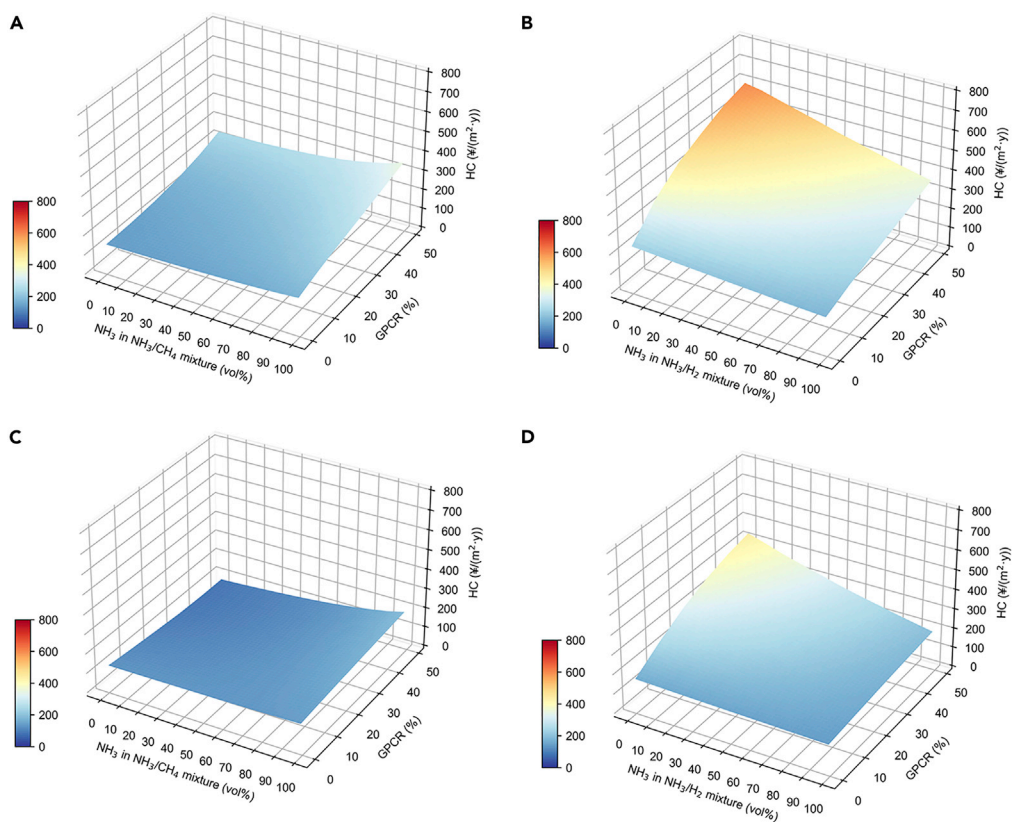
Figure 8. Heating and cooling cost per square meter from green ammonia in 2050
(A) For NH3/CH4 mixture in Harbin.
(B) For NH3/H2 mixture in Harbin.
(C) For NH3/CH4 mixture in Shenzhen.
(D) For NH3/H2 mixture in Shenzhen.

value of HC in Harbin is higher than that in Shenzhen. The HC probability density distribution is more concentrated in Shenzhen than in Harbin, indicating that HC in Harbin can be more sensitive to the fluctuation in utility price. The thick black bar in the middle indicates the interquartile range from about RMB ¥90 to 120/(m^2·y) in Shenzhen and from about RMB ¥175 to 210/(m^2·y) in Harbin.

CONCLUSIONS

The reduction of carbon emissions in fossil fuel combustion is a straight and innovative maneuver for source energy decarbonization in China, which caters to multiple forms of energy demand with minimal CO_2 emissions. Ammonia has the potential to become the primary media for achieving future peak emission and later carbon neutrality goal. Ammonia-based DES with CCHP has the potential to achieve low carbon emissions and is cost competitive according to this study. The purpose of this research is to develop a pathway for ammonia-based DES and assess its performance in emission and economy. The main findings from this study are as follows.

1) Annualized carbon emissions increase with NH_3 volume fraction and $GPCR$. On average, brown NH_3/ H_2 produces higher carbon emissions than brown NH_3/CH_4 for both Harbin and Shenzhen. The lowest annualized carbon emissions are found with zero ammonia fraction. Brown ammonia does not reduce carbon emissions as it is produced by coal gasification and the carbon emission increase as the ammonia fraction increases.

2) The HC of brown ammonia increases with NH_3 volume fraction for NH_3/CH_4 mixtures and vice versa for NH_3/H_2 mixtures. On average, the HC in Harbin is larger than that in Shenzhen for the same fuel mixture. The HC of brown NH_3/H_2 is larger than that of brown NH_3/CH_4, showing the lower competitiveness of brown NH_3/H_2 in terms of cost.
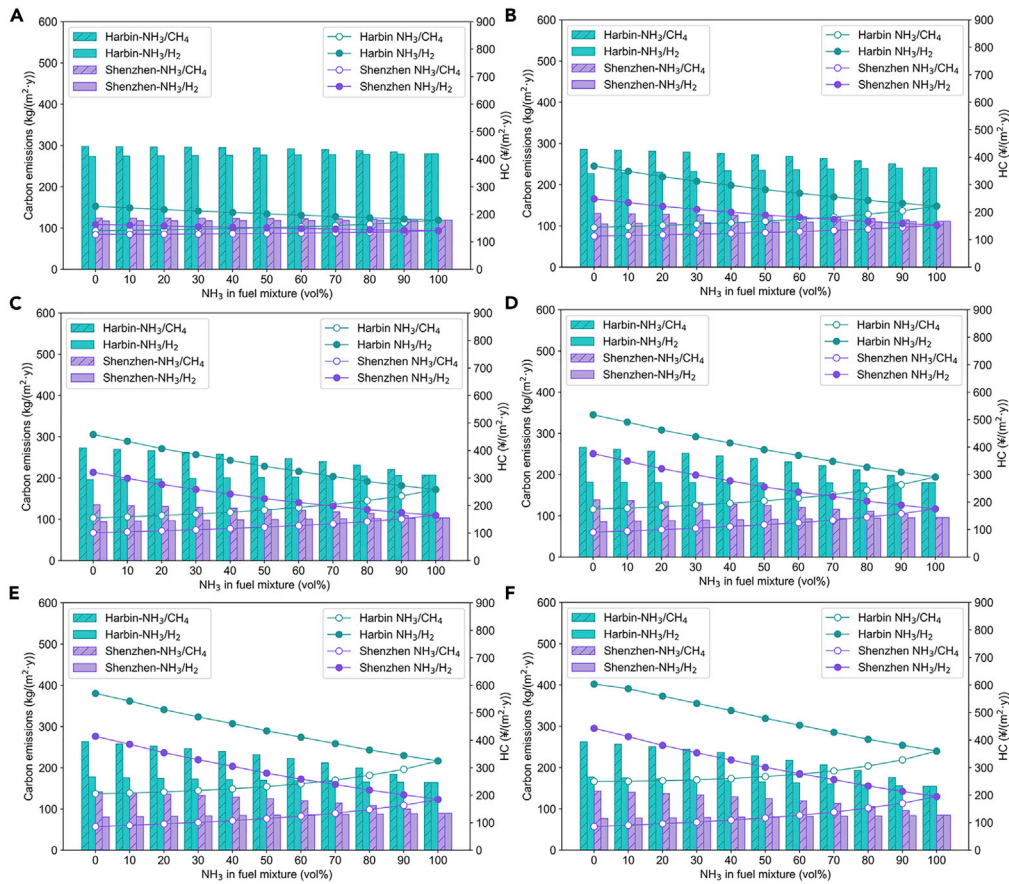
Figure 9. Carbon emissions (bars) and HC (lines) of green ammonia in 2050
(A) GPCR = 0%.
(B) GPCR = 10%.
(C) GPCR = 20%.
(D) GPCR = 30%.
(E) GPCR = 40%.
(F) GPCR = 50%.

3) Green ammonia has an outstanding decarbonization effect as carbon emissions decrease significantly with *GPCR* and NH_3 volume fraction. Except for the case of NH_3/H_2 mixtures in Shenzhen, the total carbon emission increases slightly with NH_3 volume fraction.

4) *HC* of green ammonia increases with ammonia fraction and *GPCR* for NH_3/CH_4 mixtures, while for NH_3/H_2 mixtures, *HC* increases with decreasing ammonia fraction and increasing *GPCR* for both 2022 and 2050. The *HC* of 2050 ammonia-DES is lower than that of 2022 for each case. On average, the NH_3/CH_4 mixture is more cost competitive than the NH_3/H_2 mixture both in 2022 and 2050 for Harbin and Shenzhen.

5) Compared to brown ammonia, the decarbonization trend of green ammonia becomes apparent with NH_3 volume fraction. The economic analysis shows that the *HC* of green ammonia is lower than that of brown ammonia for Harbin and Shenzhen.

6) The carbon emissions of the green NH_3/H_2 mixture are larger than those of the green NH_3/CH_4 mixture at a given NH_3 volume fraction except at 100% NH_3 volume fraction where the carbon emissions are equal. The *HC* of the green NH_3/H_2 mixture decreases with NH_3 volume fraction while the opposite trend is observed for the green NH_3/CH_4 mixture.

7) For NH_3/CH_4 mixture, NO_x emission increases and then decreases with increasing NH_3 volume fraction for a given *GPCR*. For NH_3/H_2 mixture, as the volume fraction of ammonia increases, the NO_x emission first decreases and then increases.
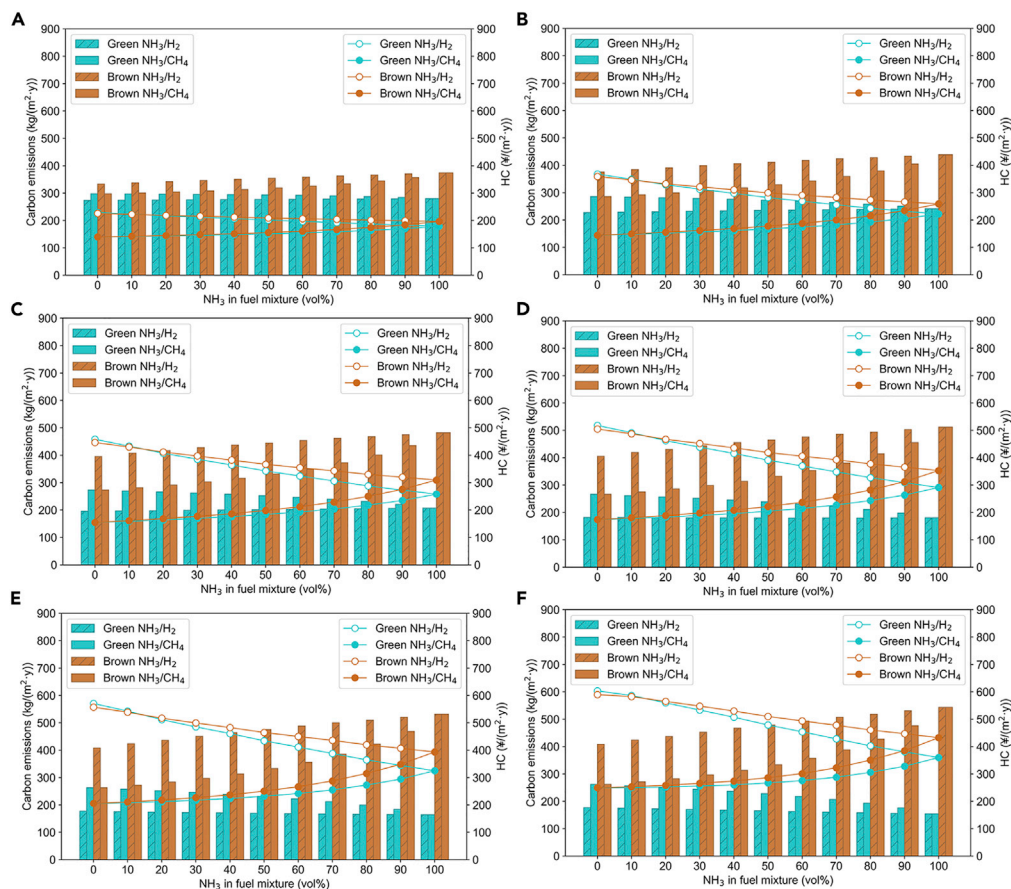
Figure 10. Carbon emissions (bars) and HC (lines) of brown ammonia and green ammonia in 2050 for Harbin
(A) GPCR = 0%.
(B) GPCR = 10%.
(C) GPCR = 20%.
(D) GPCR = 30%.
(E) GPCR = 40%.
(F) GPCR = 50%.

8) Sensitivity analysis of the effects of ammonia price, hydrogen price, methane price, and electricity price on the model *HC* shows that the electricity price is the most sensitive to the model. The *HC* has less uncertainties in Shenzhen than in Harbin.

In conclusion, green ammonia provides satisfactory decarbonization and is cost-competitive in the future. Despite the fact that the conclusions drawn by the model can be limited by certain assumptions and constraints based on existing information, the use of ammonia as an achievable and affordable energy source for DES deserves to be considered and further explored.

Limitations of the study

There are several aspects that may be further developed in future studies. It is worthy of note how the widespread use of CCHP with ammonia would influence urban NO_x levels. The NO_x emissions from ammonia-based DES presented in this study are community-wide, so it is beyond the scope of this study to consider city-wide NO_x emissions for large-scale CCHP applications using ammonia. Furthermore, the DES modeling does not take into account possible changes in the seasonal cost of renewable electricity. If wind and solar are used as renewable energy sources, then the supply of renewable electricity can change over time, causing uncertainties in carbon emission calculation.
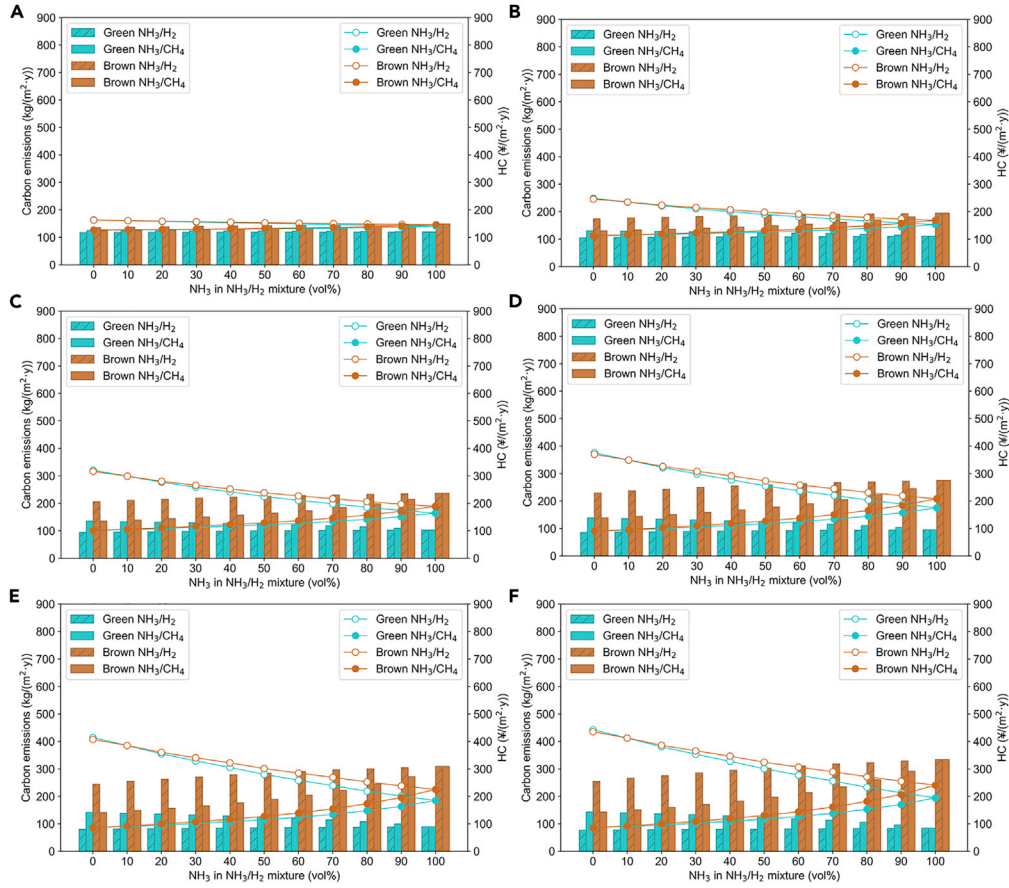
Figure 11. Carbon emissions (bars) and HC (lines) of brown ammonia and green ammonia in 2050 for Shenzhen
(A) GPCR = 0%.
(B) GPCR = 10%.
(C) GPCR = 20%.
(D) GPCR = 30%.
(E) GPCR = 40%.
(F) GPCR = 50%.

METHOD DETAILS

DES model

The hourly energy production of each combined cooling, heating, and power (CCHP) subsystem is calculated based on the coupling with the hourly building loads in the area that are simulated by building energy simulation tools. The calculation method for the energy generation of the subsystem is briefly shown in Equations (4)–(6).

$$L^i_{\text{abs,cool}} = \min\left(L^i_{\text{cool}}, L^i_{\text{plug,cool}}, L^i_{\text{gen,cool}}\right) \qquad \text{(Equation 4)}$$

$$L^i_{\text{rec,heat}} = \min\left(L^i_{\text{heat}}, L^i_{\text{plug,heat}}, L^i_{\text{gen,heat}}\right) \qquad \text{(Equation 5)}$$

$$L^i_{\text{rec,DHW}} = \min\left(L^i_{\text{DHW}}, L^i_{\text{plug,DHW}}, L^i_{\text{gen,DHW}}\right) \qquad \text{(Equation 6)}$$

$L^i_{\text{abs,cool}}$, $L^i_{\text{rec,heat}}$ and $L^i_{\text{rec,DHW}}$ are the cooling load met by the absorption chiller, the heating load met by the recovered waste heat, and the domestic hot water (DHW) heating load met by the recovered waste heat in i^{th} hour. L_{cool}, L_{heat} and L_{DHW} are the actual electricity plug load, actual Heating load and actual DHW load, respectively. This model ensures that waste heat is used first for absorption cooling, followed by space heating and DHW heating.

A

B

C

D
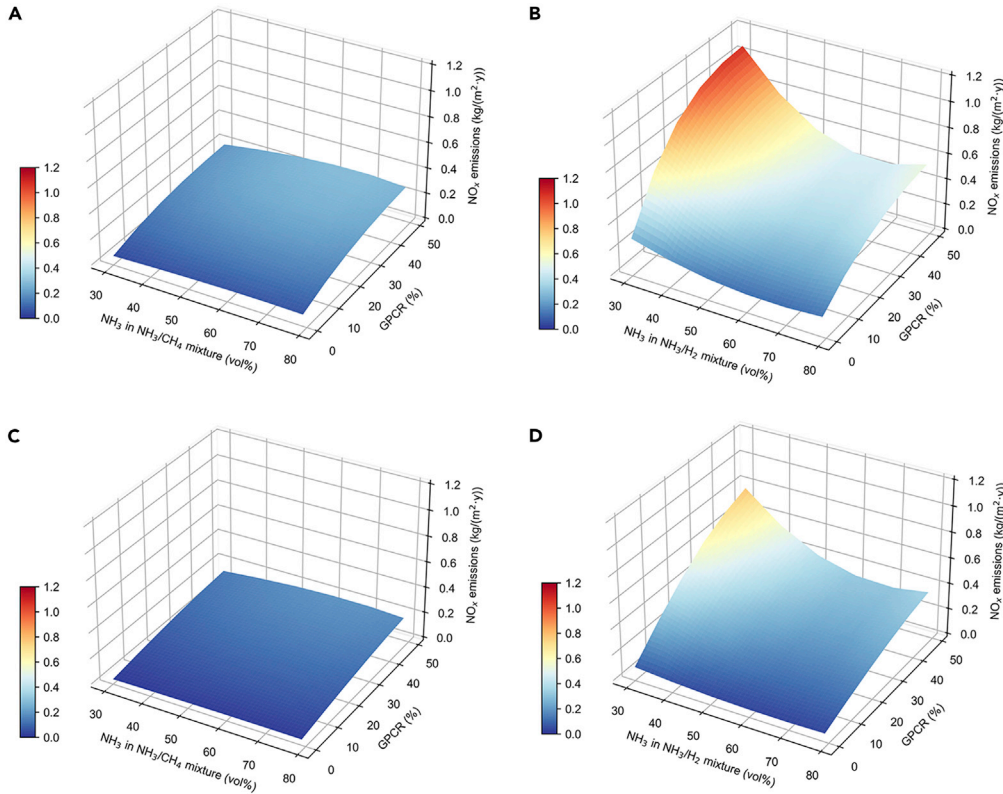
Figure 12. NOx emissions for all cases
(A) For NH3/CH4 mixture in Harbin.
(B) For NH3/H2 mixture in Harbin.
(C) For NH3/CH4 mixture in Shenzhen.
(D) For NH3/H2 mixture in Shenzhen.

Cooling load met by plug $L^i_{plug,cool}$, heating load met by plug $L^i_{plug,heat}$ and DHW heating load met by plug $L^i_{plug,DHW}$ are given as follows:

$$L^i_{plug, cool} = L^i_{plug}\left(\frac{1}{\mu_{gen}} - 1\right)\mu_{fume}COP_{abs} \qquad \text{(Equation 7)}$$

$$L^i_{plug,heat} = \left(L^i_{plug}\left(\frac{1}{\mu_{gen}} - 1\right) - \frac{L^i_{abs,cool}}{\mu_{fume}COP_{abs}}\right)\mu_{exch} \qquad \text{(Equation 8)}$$

$$L^i_{plug,DHW} = \left(L^i_{plug}\left(\frac{1}{\mu_{gen}} - 1\right) - \frac{L^i_{abs,cool}}{\mu_{fume}COP_{abs}} - \frac{L^i_{rec,heat}}{\mu_{exch}}\right)\mu_{exch} \qquad \text{(Equation 9)}$$

where L_{plug} is the actual electricity plug load, μ_{gen} is the efficiency of the generator, μ_{fume} is the efficiency of the waste fume capturing, COP_{abs} is the coefficient of performance of the absorption chiller, μ_{exch} is the efficiency of the plate heat exchanger.

Cooling load met by generator $L^i_{gen,cool}$, heating load met by generator $L^i_{gen,heat}$ and DHW heating load met by generator $L^i_{gen,DHW}$ are given as follows:

$$L^i_{gen,cool} = P^{max}_{gen}\left(\frac{1}{\mu_{gen}} - 1\right)\mu_{fume}COP_{abs} \qquad \text{(Equation 10)}$$
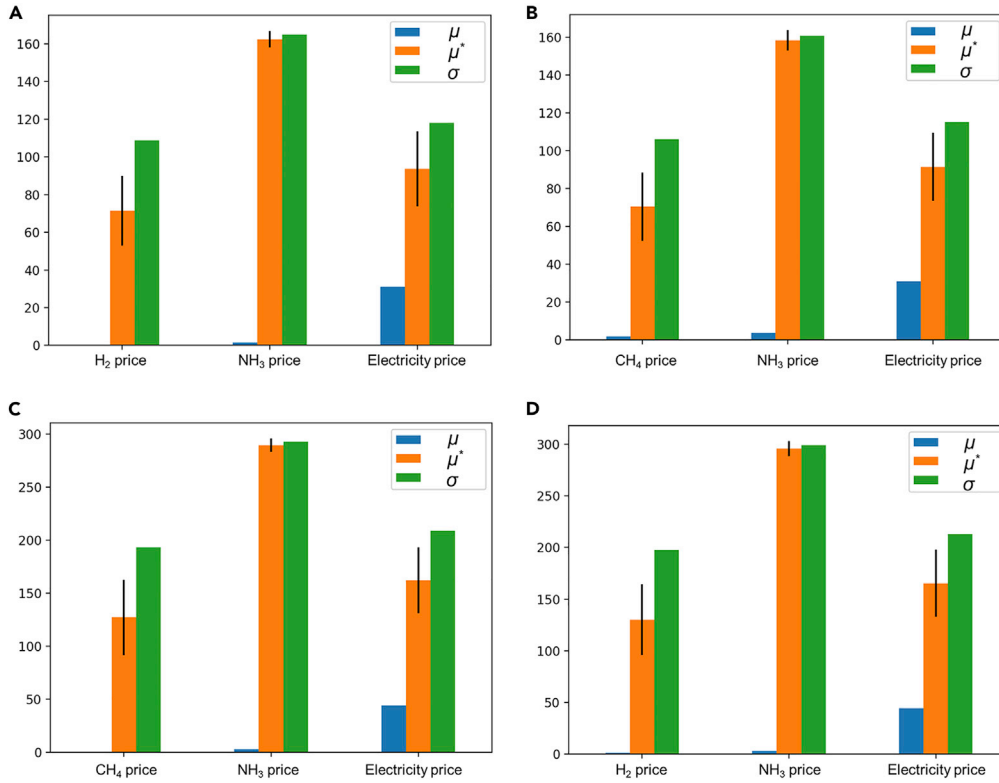
Figure 13. The influence of economic parameters on the HC for green ammonia in 2050
(A) For NH3/CH4 mixture in Harbin.
(B) For NH3/H2 mixture in Harbin.
(C) For NH3/CH4 mixture in Shenzhen.
(D) For NH3/H2 mixture in Shenzhen.

$$L_{\text{gen,heat}}^{i} = \left(P_{\text{gen}}^{\max} \left(\frac{1}{\mu_{\text{gen}}} - 1 \right) - \frac{L_{\text{abs,cool}}^{i}}{\mu_{\text{fume}} COP_{\text{abs}}} \right) \mu_{\text{exch}} \qquad \text{(Equation 11)}$$

$$L_{\text{gen,DHW}}^{i} = \left(P_{\text{gen}}^{\max} \left(\frac{1}{\mu_{\text{gen}}} - 1 \right) - \frac{L_{\text{abs,cool}}^{i}}{\mu_{\text{fume}} COP_{\text{abs}}} - \frac{L_{\text{rec,heat}}^{i}}{\mu_{\text{exch}}} \right) \mu_{\text{exch}} \qquad \text{(Equation 12)}$$

where $P_{\text{gen}}^{\max}$ is the maximum gas generator output power which is calculated as $P_{\text{gen}}^{\max} = \max(L_{\text{plug}}^{i=1}, L_{\text{plug}}^{i=2}, \cdots, L_{\text{plug}}^{i=8760}) r_{\text{gen}}$, r_{gen} is the ratio of gas generator output power to the peak electricity power load.

Economic performance

To evaluate the economic performance of the DES, annualized life cycle heating and cooling cost per square meter (*HC*) is selected to be the objective function. This optimization model obtains the optimized DES configuration by minimizing the *HC* as follows:

$$HC_y = \frac{IC_{\text{total}} {}^{*}(1+y) + \sum_{i}^{8760} \left(U_{\text{grid, plug}}^{i} P_{\text{elec}}^{i} \right) - R_{\text{elec}} + C_{\text{hc\_purchase}}}{A} \qquad \text{(Equation 13)}$$

where HC_y is the life cycle fee that the clients in the buildings have to pay for their heating and cooling under a certain life cycle profit rate y, IC_{total} is the total investment cost, $U_{\text{grid, plug}}^{i}$ is the grid purchase for plug load in i^{th} hour, P_{elec}^{i} is the electricity purchase price in i^{th} hour, R_{elec} is the revenue of the electricity, $C_{\text{hc\_puchase}}$ is the cost of purchased heating and cooling. All calculations are based on the current exchange rate of 6.36:1 for the RMB to USD and 6.93:1 for the RMB to EUR. The price of methane remains constant owing to the extraction of methane mainly from natural gas. Owing to the abundance of renewable
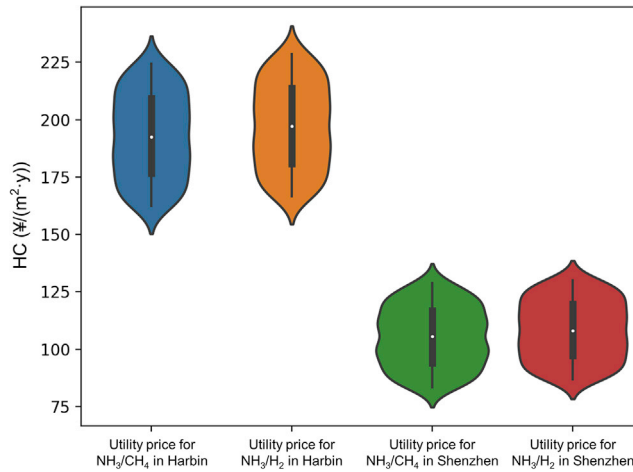
Figure 14. HC change scenarios for green ammonia in 2050

resources and coal in Inner Mongolia, the fuel supply location is assumed to be in Inner Mongolia, China, for the study to be representative and to facilitate the modeling. For simplicity and ease of clarification, hydrogen and ammonia production and transportation costs are variable, while methane costs are assumed to remain constant through the future from natural gas production.

The cost per unit capacity of each part of the CCHP system is shown in Table 2.

This study aims to optimize the CCHP system by adjusting the value of generator power capacity ratio *GPCR* (the ratio of gas generator output power to the peak electricity power load), which is set from 0 to 0.5. The volume share of ammonia in the fuel mixture in the model ranges from 0% to 100%. The optimization objective is to minimize the cooling and heating fee paid by end users at a life cycle profit rate of 15%.

The constraints that need to be satisfied for this CCHP system are shown below:

$$L^{i}_{\text{abs, cool}} + L^{i}_{\text{reg, cool}} \geq L^{i}_{\text{cool}} \qquad \text{(Equation 14)}$$

$$L^{i}_{\text{rec, heat}} + L^{i}_{\text{rec,DHW}} + L^{i}_{\text{boiler}} \geq L^{i}_{\text{heat}} + L^{i}_{\text{DHW}} \qquad \text{(Equation 15)}$$

$$0 \leq r_{\text{gen}} \leq 0.5 \qquad \text{(Equation 16)}$$

where $L_{\text{reg, cool}}$ is the cooling load met by the regular chiller, L_{boiler} is the heating load met by the boiler.

Emissions

Based on the optimized *HC*, the carbon emissions of the operational phase of the building can be obtained. There are three main sources of carbon emissions from the buildings studied in this article namely (1) the production of electricity from power plants, (2) the production and transport of ammonia, hydrogen, and methane. Therefore, the formula for annualized CE_{total} can be expressed as follows:

$$CE_{\text{total}} = CE_{\text{elec}} + CE_{\text{gas}} \qquad \text{(Equation 17)}$$

where CE_{total} is the carbon emissions of all parts, CE_{elec} is the carbon emissions generated during the production and use of electricity, CE_{gas} is the carbon emissions from the mixture of gases consumed by the DES system, which is calculated as:

$$CE_{\text{elec}} = E_{\text{purchase}}(\eta_{\text{fossil}} CF_{\text{fossil}} + \eta_{\text{renewable}} CF_{\text{renewable}})/A \qquad \text{(Equation 18)}$$

where E_{purchase} is the total purchased electricity from the grid, η_{fossil} and $\eta_{\text{renewable}}$ is the volume fraction of fossil energy and renewable energy and renewable energy, respectively, CF_{fossil} and $CF_{\text{renewable}}$ are the carbon footprint fossil-based power generation and renewable-based power generation, respectively, A is the total building floor area of the project.

Table 2. Cost per unit capacity of each part

Item	Cost	Unit
Regular Chiller Unit Cost	500	¥/kW
Boiler Unit Cost	100	¥/kW
Generator Unit Cost	9,000	¥/kW
Storage Battey Unit Cost	1,200	¥/kWh
Grid Distribution Unit Cost	1,500	¥/kVA
Absorption Chiller Unit Cost	400	¥/kW

Carbon emissions from gas include gas production and transportation as well as carbon from combustion, if any. Carbon emissions from the storage process are ignored because the model assumes *in situ* use. Carbon emissions from NH_3/H_2 mixtures are calculated as:

$$CE_{gas} = (CE_{NH_3} + CE_{H_2})/A \qquad \text{(Equation 19)}$$

$$CE_{NH_3} = V_{gas}\eta_{NH_3}\rho_{NH_3}(CF_{NH_3,production} + CF_{NH_3,transportation}) \qquad \text{(Equation 20)}$$

$$CE_{H_2} = V_{gas}\eta_{H_2}\rho_{H_2}(CF_{H_2,production} + CF_{H_2,transportation}) \qquad \text{(Equation 21)}$$

where CE_{NH_3} and CE_{H_2} are carbon emissions from ammonia and hydrogen, respectively, V_{gas} is the mixture of gases consumed by the DES system, η_{NH_3} and η_{H_2} are volume fraction of ammonia and hydrogen, respectively, ρ_{NH_3} and are the densities of ammonia and hydrogen, respectively, at standard condition, $CF_{NH_3,production}$ and $CF_{NH_3,transportation}$ are the carbon footprint of ammonia production and transportation, respectively, $CF_{H_2,production}$ and $CF_{H_2,transportation}$ are the carbon footprint of hydrogen production and transportation, respectively.

η_{NH_3} and η_{H_2} are calculated as:

$$\eta_{NH_3} = \frac{V_{NH_3}}{V_{NH_3} + V_{H_2}} \times 100\% \qquad \text{(Equation 22)}$$

$$\eta_{H_2} = \frac{V_{H_2}}{V_{NH_3} + V_{H_2}} \times 100\% \qquad \text{(Equation 23)}$$

Carbon emissions from NH_3/CH_4 mixtures are calculated as:

$$CE_{gas} = (CE_{NH_3} + CE_{CH_4})/A \qquad \text{(Equation 24)}$$

$$CE_{CH_4} = V_{gas}\eta_{CH_4}\rho_{CH_4}(CF_{CH_4,production} + CF_{CH_4,transportation} + CF_{CH_4,combustion}) \qquad \text{(Equation 25)}$$

where η_{CH_4} is the volume fraction of methane, ρ_{CH_4} is the density of methane at standard condition, $CF_{CH_4,production}$, $CF_{CH_4,transportation}$ and $CF_{CH_4,combustion}$ are carbon footprint for methane production, transportation and combustion, respectively. The carbon emissions of methane, ammonia, and hydrogen are set to be constant from 2020 to 2050 for the purpose of clarification and comparison. η_{CH_4} is calculated as:

$$\eta_{CH_4} = \frac{V_{CH_4}}{V_{NH_3} + V_{CH_4}} \times 100\% \qquad \text{(Equation 26)}$$

As ammonia is a nitrogenous fuel, nitrogen oxide emissions are another major issue. As the nitrogen dioxide content is almost zero, the NO_x emission in the model is mainly NO. The annualized NO_x emissions are shown in Equation (27).

$$NE = (V_{gas}\eta_{NO_x}\rho_{NO_x}/1000000)/A \qquad \text{(Equation 27)}$$

where NE is the nitrogen oxide emissions, η_{NO_x} is the volume fraction (ppm) of NO_x, ρ_{NO_x} is the density of NO_x at standard condition. NO_x is considered only from the combustion process, therefore, there is no difference in NO_x emissions from green and brown ammonia.

Table 3. Model assumptions

Item	Unit	Value(s)
Project lifetime	Years	15
Profit rate	%	15
Discount rate	%	5%
Regular chiller COP		5
Ratio of storage battery capacity to peak electricity power load		0.05
Absorption chiller COP		1.2
Rectifier efficiency	%	95
Commercial charging pile number		100
Plate exchanger efficiency	%	95
Fume capturing efficiency	%	90
Distance from energy production to end users (Harbin)	km	1,700
Distance from energy production to end users (Shenzhen)	km	2,400

For simplicity and clarification, the model makes the following assumptions:

- The hourly electricity selling price in Shenzhen and Harbin remains constant from 2022 to 2050.

- The price of methane remains constant.

- The cost per unit capacity of each part of the CCHP system keep constant from 2022 to 2050.

- The community's cooling, heating, and electricity loads are the same in 2022 and 2050.

- The analysis does not take into account the change in the efficiency of various devices from 2022 to 2050, such as boilers and gas turbines.

- The carbon footprint and the share of electricity generation remain unchanged from 2022 to 2050.

In this study, the main criteria for evaluating CCHP systems are economic performance and environmental performance. To achieve the optimization of the objectives, two fuel mixtures, NH_3/H_2 and NH_3/CH_4, were used in this study. The costing of fuel takes into account the cost of the production and transportation sections, and the cost of storage is ignored owing to the assumption that the fuel is used *in situ*. Based on the analysis in the article, the following assumptions were made for the model parameters of the CCHP system in Table 3.

SUPPLEMENTAL INFORMATION

Supplemental information can be found online at https://doi.org/10.1016/j.isci.2022.105120.

AUTHOR CONTRIBUTIONS

Conceptualization, L.Z. and P.S.; Methodology, H.D., P.S., and L.Z.; Investigation, H.D., P.S., W.C., D.N., C.S., and L.Z.; Writing – Original Draft, H.D. and P.S.; Writing – Review & Editing, H.D., P.S. W.C., D.N., C.S., and L.Z.; Supervision, L.Z. and P.S.; Funding acquisition, L.Z. and P.S.

DECLARATION OF INTERESTS

The authors declare no competing interests.

REFERENCES

Agreement, P. (2015). Paris Agreement (HeinOnline), p. 2017.

Al-Breiki, M., and Bicer, Y. (2021). Comparative life cycle assessment of sustainable energy carriers including production, storage, overseas transport and utilization. J. Cleaner Prod. *279*, 123481.

Association, C.B.E. (2021). China building energy research report 2020. Build. Energy Efficiency *49*, 1–6.

Bao, Y., Du, H., Chai, W.S., Nie, D., and Zhou, L. (2022). Numerical investigation and optimization on laminar burning velocity of ammonia-based fuels based on GRI3.0 mechanism. Fuel *318*, 123681. https://doi.org/10.1016/j.fuel.2022. 123681.

Beccali, M., Cellura, M., Fontana, M., Longo, S., and Mistretta, M. (2013). Energy retrofit of a single-family house: life cycle net energy saving and environmental benefits. Renew. Sustain. Energy Rev. *27*, 283–293.

Bicer, Y., and Dincer, I. (2017). Life cycle assessment of nuclear-based hydrogen and ammonia production options: a comparative evaluation. Int. J. Hydrogen Energy *42*, 21559–21570.

Bicer, Y., and Dincer, I. (2018). Clean fuel options with hydrogen for sea transportation: a life cycle approach. Int. J. Hydrogen Energy *43*, 1179–1193.

Boero, A.J., Kardux, K., Kovaleva, M., Salas, D.A., Mooijer, J., Mashruk, S., Townsend, M., Rouwenhorst, K., Valera-Medina, A., and Ramirez, A.D. (2021). Environmental life cycle assessment of ammonia-based electricity. Energies *14*, 6721. https://doi.org/10.3390/en14206721.

Cardoso, J.S., Silva, V., Rocha, R.C., Hall, M.J., Costa, M., and Eusébio, D. (2021). Ammonia as an energy vector: current and future prospects for low-carbon fuel applications in internal combustion engines. J. Clean. Prod. *296*, 126562.

Cesaro, Z., Ives, M., Nayak-Luke, R., Mason, M., and Bañares-Alcántara, R. (2021). Ammonia to power: forecasting the levelized cost of electricity from green ammonia in large-scale power plants. Appl. Energy *282*, 116009.

Chai, W.S., Bao, Y., Jin, P., Tang, G., and Zhou, L. (2021). A review on ammonia, ammonia-hydrogen and ammonia-methane fuels. Renew. Sustain. Energy Rev. *147*, 111254. https://doi.org/10.1016/j.rser.2021.111254.

China Southern Power Grid Ltd. (2022). Shenzhen Residential Electricity Price List. https://95598.csg.cn/#/sz/serviceInquire/LRLayer/elePriceInquire.

Commission, H.P.D.a.R. (2022). On further improving the peak and valley tariff policy measures. http://fgw.harbin.gov.cn/art/2022/3/11/art_24909_1238284.html.

Council, I.C., Officials, B., International, C.A., Officials, I.C.o.B., and International, S.B.C.C. (2000). International Energy Conservation Code (International Code Council).

Crawley, D.B., Lawrie, L.K., Pedersen, C.O., and Winkelmann, F.C. (2000). Energy plus: energy simulation program. ASHRAE J. *42*, 49–56.

Arnaiz del Pozo, C., and Cloete, S. (2022). Techno-economic assessment of blue and green ammonia as energy carriers in a low-carbon future. Energy Convers. Manag. *255*, 115312.

Di Lullo, G., Oni, A.O., Gemechu, E., and Kumar, A. (2020). Developing a greenhouse gas life cycle assessment framework for natural gas transmission pipelines. J. Nat. Gas Sci. Eng. *75*, 103136.

Fan, J.-L., Yu, H., and Wei, Y.-M. (2015). Residential energy-related carbon emissions in urban and rural China during 1996–2012: from the perspective of five end-use activities. Energy Build. *96*, 201–209.

Fasihi, M., Weiss, R., Savolainen, J., and Breyer, C. (2021). Global potential of green ammonia based on hybrid PV-wind power plants. Appl. Energy *294*, 116170.

Franco, M.C., Rocha, R.C., Costa, M., and Yehia, M. (2021). Characteristics of NH3/H2/air flames in a combustor fired by a swirl and bluff-body stabilized burner. Proc. Combust. Inst. *38*, 5129–5138.

Gálvez, M., Halmann, M., and Steinfeld, A. (2007). Ammonia production via a two-step Al2O3/AlN thermochemical cycle. 1. Thermodynamic, environmental, and economic analyses. Indus. Eng. Chem. Res. *46*, 2042–2046.

Ghorbani, B., Mehrpooya, M., and Sadeqi, M. (2021). Thermodynamic and exergy evaluation of a novel integrated structure for generation and store of power and refrigeration using ammonia-water mixture CCHP cycle and energy storage systems. Sustain. Energy Technol. Assessments *47*, 101329.

Giddey, S., Badwal, S., Munnings, C., and Dolan, M. (2017). Ammonia as a renewable energy transportation media. ACS Sustain. Chem. Eng. *5*, 10231–10239.

Gill, S.S., Chatha, G.S., Tsolakis, A., Golunski, S.E., and York, A.P.E. (2012). Assessing the effects of partially decarbonising a diesel engine by co-fuelling with dissociated ammonia. Int. J. Hydrogen Energy *37*, 6074–6083. https://doi.org/10.1016/j.ijhydene.2011.12.137.

Gu, Y., Chen, Q., Xue, J., Tang, Z., Sun, Y., and Wu, Q. (2020). Comparative techno-economic study of solar energy integrated hydrogen supply pathways for hydrogen refueling stations in China. Energy Convers. Manag. *223*, 113240.

Guteša Božo, M., Mashruk, S., Zitouni, S., and Valera-Medina, A. (2021). Humidified ammonia/hydrogen RQL combustion in a trigeneration gas turbine cycle. Energy Convers. Manag. *227*, 113625. https://doi.org/10.1016/j.enconman.2020.113625.

Ishaq, H., and Dincer, I. (2020). A comprehensive study on using new hydrogen-natural gas and ammonia-natural gas blends for better performance. J. Nat. Gas Sci. Eng. *81*, 103362. https://doi.org/10.1016/j.jngse.2020.103362.

Ishihara, S., Zhang, J., and Ito, T. (2020). Numerical calculation with detailed chemistry of effect of ammonia co-firing on NO emissions in a coal-fired boiler. Fuel *266*, 116924.

Janssen, J.L., Weeda, M., Detz, R.J., and van der Zwaan, B. (2022). Country-specific cost projections for renewable hydrogen production through off-grid electricity systems. Appl. Energy *309*, 118398.

Kim, S.-i., Kwak, H.-g., and Yang, W. (2021). Process simulation of the effect of ammonia co-firing on the supercritical boiler system for reduction of greenhouse gas. J. Korean Soc. Combust. *26*, 1–12. https://doi.org/10.15231/jksc.2021.26.4.001.

Kurata, O., Iki, N., Matsunuma, T., Inoue, T., Tsujimura, T., Furutani, H., Kobayashi, H., and Hayakawa, A. (2017). Performances and emission characteristics of NH3–air and NH3CH4–air combustion gas-turbine power generations. Proc. Combust. Inst. *36*, 3351–3359. https://doi.org/10.1016/j.proci.2016.07.088.

Liu, W., Wan, Y., Xiong, Y., and Gao, P. (2022). Green hydrogen standard in China: standard and evaluation of low-carbon hydrogen, clean hydrogen, and renewable hydrogen. Int. J. Hydrogen Energy *47*, 24584–24591. https://doi.org/10.1016/j.ijhydene.2021.10.193.

MacFarlane, D.R., Cherepanov, P.V., Choi, J., Suryanto, B.H., Hodgetts, R.Y., Bakker, J.M., Ferrero Vallana, F.M., and Simonov, A.N. (2020). A roadmap to the ammonia economy. Joule *4*, 1186–1205. https://doi.org/10.1016/j.joule.2020.04.004.

Morris, M.D. (1991). Factorial sampling plans for preliminary computational experiments. Technometrics *33*, 161–174.

Murai, R., Omori, R., Kano, R., Tada, Y., Higashino, H., Nakatsuka, N., Hayashi, J., Akamatsu, F., Iino, K., and Yamamoto, Y. (2017). The radiative characteristics of NH3/N2/O2 non-premixed flame on a 10 kW test furnace. Energy Proc. *120*, 325–332.

Nayak-Luke, R.M., and Bañares-Alcántara, R. (2020). Techno-economic viability of islanded green ammonia as a carbon-free energy vector and as a substitute for conventional production. Energy Environ. Sci. *13*, 2957–2966.

Nozari, H., and Karabeyoğlu, A. (2015). Numerical study of combustion characteristics of ammonia as a renewable fuel and establishment of reduced reaction mechanisms. Fuel *159*, 223–233. https://doi.org/10.1016/j.fuel.2015.06.075.

Oni, A.O., Anaya, K., Giwa, T., Di Lullo, G., and Kumar, A. (2022). Comparative assessment of blue hydrogen from steam methane reforming, autothermal reforming, and natural gas decomposition technologies for natural gas-producing regions. Energy Convers. Manag. *254*, 115245. https://doi.org/10.1016/j.enconman.2022.115245.

Osorio-Tejada, J., Tran, N.N., and Hessel, V. (2022). Techno-environmental assessment of small-scale Haber-Bosch and plasma-assisted ammonia supply chains. Sci. Total Environ. *826*, 154162.

Otomo, J., Koshi, M., Mitsumori, T., Iwasaki, H., and Yamada, K. (2018). Chemical kinetic modeling of ammonia oxidation with improved reaction mechanism for ammonia/air and ammonia/hydrogen/air combustion. Int. J. Hydrogen Energy 43, 3004–3014.

Parikhani, T., Azariyan, H., Behrad, R., Ghaebi, H., and Jannatkhah, J. (2020). Thermodynamic and thermoeconomic analysis of a novel ammonia-water mixture combined cooling, heating, and power (CCHP) cycle. Renew. Energy 145, 1158–1175.

Rocha, R.C., Ramos, C.F., Costa, M., and Bai, X.-S. (2019). Combustion of NH3/CH4/air and NH3/H2/air mixtures in a porous burner: experiments and kinetic modeling. Energy Fuels 33, 12767–12780. https://doi.org/10.1021/acs.energyfuels.9b02948.

Roos, T.H. (2021). The cost of production and storage of renewable hydrogen in South Africa and transport to Japan and EU up to 2050 under different scenarios. Int. J. Hydrogen Energy 46, 35814–35830.

Salmon, N., and Bañares-Alcántara, R. (2021). Green ammonia as a spatial energy vector: a review. Sustain. Energy Fuels 5, 2814–2839. https://doi.org/10.1039/d1se00345c.

Shi, X., Qian, Y., and Yang, S. (2020). Fluctuation analysis of a complementary wind–solar energy system and integration for large scale hydrogen production. ACS Sustain. Chem. Eng. 8, 7097–7110.

Smith, C., Hill, A.K., and Torrente-Murciano, L. (2020). Current and future role of Haber–Bosch ammonia in a carbon-free energy landscape. Energy Environ. Sci. 13, 331–344.

Standards, N.I.o., and Technology. (2017). NIST Chemistry WebBook, SRD 69—Thermophysical Properties of Fluid Systems.

State Grid Heilongjiang Electric Power Co, L. (2021). Heilongjiang Power Grid Sales Tariff. http://www.hl.sgcc.com.cn/html/main/col1014/2017-03/28/20170328151908984171689_1.html.

Tamura, M., Gotou, T., Ishii, H., and Riechelmann, D. (2020). Experimental investigation of ammonia combustion in a bench scale 1.2 MW-thermal pulverised coal firing furnace. Appl. Energy 277, 115580.

Tang, G., Jin, P., Bao, Y., Chai, W.S., and Zhou, L. (2021). Experimental investigation of premixed combustion limits of hydrogen and methane additives in ammonia. Int. J. Hydrogen Energy 46, 20765–20776.

Theuri, D. (2008). Solar and Wind Energy Resource Assessment. Kenya Country Report (SWERA Project).

Tian, Z., Li, Y., Zhang, L., Glarborg, P., and Qi, F. (2009). An experimental and kinetic modeling study of premixed NH3/CH4/O2/Ar flames at low pressure. Combust. Flame 156, 1413–1426.

Valera-Medina, A., Gutesa, M., Xiao, H., Pugh, D., Giles, A., Goktepe, B., Marsh, R., and Bowen, P. (2019). Premixed ammonia/hydrogen swirl combustion under rich fuel conditions for gas turbines operation. Int. J. Hydrogen Energy 44, 8615–8626. https://doi.org/10.1016/j.ijhydene.2019.02.041.

Valera-Medina, A., Marsh, R., Runyon, J., Pugh, D., Beasley, P., Hughes, T., and Bowen, P. (2017a). Ammonia–methane combustion in tangential swirl burners for gas turbine power generation. Appl. Energy 185, 1362–1371.

Valera-Medina, A., Morris, S., Runyon, J., Pugh, D.G., Marsh, R., Beasley, P., and Hughes, T. (2015). Ammonia, methane and hydrogen for gas turbines. Energy Proc. 75, 118–123. https://doi.org/10.1016/j.egypro.2015.07.205.

Valera-Medina, A., Pugh, D., Marsh, P., Bulat, G., and Bowen, P. (2017b). Preliminary study on lean premixed combustion of ammonia-hydrogen for swirling gas turbine combustors. Int. J. Hydrogen Energy 42, 24495–24503.

Wang, Z., Han, W., Zhang, N., Liu, M., and Jin, H. (2017). Proposal and assessment of a new CCHP system integrating gas turbine and heat-driven cooling/power cogeneration. Energy Convers. Manag. 144, 1–9.

Wu, C., Zheng, S., Wang, Z., Chen, R., Hu, X., and Chen, J. (2021). Discussion on ammonia as one of the energy storage media of solar energy in China. Energy Strategy Rev. 38, 100697.

Xiao, H., Valera-Medina, A., and Bowen, P.J. (2017). Study on premixed combustion characteristics of co-firing ammonia/methane fuels. Energy 140, 125–135.

Yapicioglu, A., and Dincer, I. (2018). Performance assesment of hydrogen and ammonia combustion with various fuels for power generators. Int. J. Hydrogen Energy 43, 21037–21048.

Zhang, J., Ito, T., Ishii, H., Ishihara, S., and Fujimori, T. (2020). Numerical investigation on ammonia co-firing in a pulverized coal combustion facility: effect of ammonia co-firing ratio. Fuel 267, 117166.

Zhang, J., Meerman, H., Benders, R., and Faaij, A. (2021). Techno-economic and life cycle greenhouse gas emissions assessment of liquefied natural gas supply chain in China. Energy 224, 120049. https://doi.org/10.1016/j.energy.2021.120049.

Zhang, Y., Li, X., Li, Q., Bulle, C., Hua, H., Jiang, S., and Liu, X. (2019). Intensive carbon dioxide emission of coal chemical industry in China. J. Hand Surg. Eur. 44, 540–541.

Zhao, X., Cai, Q., Zhang, S., and Luo, K. (2017). The substitution of wind power for coal-fired power to realize China's CO2 emissions reduction targets in 2020 and 2030. Energy 120, 164–178. https://doi.org/10.1016/j.energy.2016.12.109.

Zhou, Z., Liu, P., Li, Z., and Ni, W. (2013). An engineering approach to the optimal design of distributed energy systems in China. Appl. Therm. Eng. 53, 387–396. https://doi.org/10.1016/j.applthermaleng.2012.01.067.